

Photo-crosslinked nanofibers of poly(ether amine) (PEA) for the ultrafast separation of dyes through molecular filtration†

Cite this: *Polym. Chem.*, 2014, 5, 2027

Guangxia Fu, Zhilong Su, Xuesong Jiang* and Jie Yin

Molecular filtration is very attractive in the industrial applications of separation and water treatment, but it is challenging to realize fast separation due to the low transport rates and filtrate loss within the membranes in commercial ultrafiltration. We here demonstrated a novel example that a nanofiber membrane of poly(ether amine) (PEA) can be used in the separation of hydrophilic dyes through fast molecular filtration. Two types of PEA nanofiber membrane (PEA-NF) were fabricated through the electrospinning process, which were further photo-crosslinked through the UV-induced dimerization of coumarin groups. Regardless of their charge state, the obtained PEA-NF membranes exhibited strong adsorption to Ponceau S (PS), Rose Bengal (RB), Orange G (OG), Ponceau SX (PSX), and Bismarck brown Y (BY), and with weak adsorption to Methylene Blue trihydrate (MB), and Rhodamine 6G (R6G). Based on the unique selective adsorption to the hydrophilic dyes, PEA-NF membranes can separate mixtures of PS/MB in aqueous solution through molecular filtration with a very high flux rate of $2870 \text{ L m}^{-2} \text{ h}^{-1}$. In addition, the PEA-NF membranes are easily regenerated and keep the high separation efficiency over ten adsorption–washing cycles. The integration of the fast separation, easy regeneration and low-cost give PEA-NF membranes potential applications such as separation and water purification.

Received 17th October 2013
Accepted 8th November 2013

DOI: 10.1039/c3py01443f

www.rsc.org/polymers

1. Introduction

Ultrafiltration and nanofiltration technology derived from the conventional separation method of filtration, can be applied to separate mixtures by their molecule weights at a molecular level ($<10^6$ Da for ultrafiltration and $<10^3$ Da for nanofiltration).^{1,2} As an emerging area of great interest in separation,³ molecular filtration is based on the membrane's high selectivity, which is the key factor to filter molecules with a high flux.^{4–8} The selectivity is dependent on the chemical features of the membrane,^{9–13} provides the possibility of a membrane to separate mixtures with molecules of nearly the same size¹⁴ through molecular filtration, which makes the membranes very promising in the fields such as water treatment,^{15,16} gas separation,^{17,18} purifying of drug molecules and biomolecules,^{19,20} and organics recycling.^{21,22}

Recently, membranes made of nanofibers have attracted much attention in the field of molecular filtration.^{23–25} Nanofiber membranes benefit the applications of adsorption and separation because they are advantageous in offering huge

surface to volume ratios, uniform pore-size distribution, convenient recycling, and high equilibrium adsorption capacity.^{26–28} As for the nanofiber membranes, flux and selectivity are two crucial factors to determine their performance.^{29–33} Usually, high selectivity is controlled by the surface properties of the nanofiber membrane which discriminates the type of species passing through it, resulted from the interaction between filter and filtrate³⁴ such as hydrogen-bonding,³⁵ ionic-bonding^{36–38} and host–guest interactions.¹² Yu and Uyar's groups reported that nanofibers functionalized with cyclodextrins were used to remove dye molecules from aqueous solution through molecular filtration.^{12,39,40} In these reports, however, no investigation was done on the selectivity of these nanofiber membranes, which were not applicable to separate dye mixtures in aqueous solution. In addition, the limitation of low flux could restrict molecular filtration in the field of separation to some extent.⁴¹ Thus, it is very promising to develop a kind of nanofiber membrane which can separate mixtures of molecules in solution with high selectivity and high flux.¹¹

Based on the unique selective adsorption of poly(ether amine) (PEA) hydrogel to dyes, we here demonstrated a novel example of nanofiber membranes of PEA for separation of dyes through molecular filtration. We wanted to combine the unique selectivity of PEA and the superiority of nanofiber membrane in the simple filtration approach to achieve an efficient separation. Materials based on poly(ether amine) (PEA) such as nanogel, microgel and hydrogel developed by our group recently,

School of Chemistry & Chemical Engineering, State Key Laboratory for Metal Matrix Composite Materials, Shanghai Jiao Tong University, Shanghai 200240, People's Republic of China. E-mail: ponygle@sjtu.edu.cn; Fax: +86-21-54747445; Tel: +86-21-54743268

† Electronic supplementary information (ESI) available. See DOI: 10.1039/c3py01443f

exhibited the unique selective adsorption to dyes, which provides an important alternative in smart separation.^{42–45} In this text, we prepared the photo-crosslinked nanofibers of PEA (PEA-NF) through electrospinning, and then systematically investigated the interaction between PEA-NF and hydrophilic dyes. PEA-NF is resistant to solvent and exhibited selective adsorption to dyes. Moreover, PEA-NF membrane can separate a dyes' mixture through facile filtration with a very high flux of $2870 \text{ L m}^{-2} \text{ h}^{-1}$, and can keep the high efficiency in separation even after ten times of regeneration cycles.

2. Results and discussion

Fabrication and characterization of PEA-NF membranes

As shown in Fig. 1a, two types of linear poly(ether amine) containing coumarin moieties in the backbone (PEA and SA-PEA) were used to fabricate the nanofiber membranes through electrospinning. Due to the well-known performance of photo-dimerization, the incorporation of coumarin will provide the ability of the nanofiber membrane to be photo-crosslinked by irradiation of UV-light. The obtained cross-linked nanofiber membrane is expected to be resistant to solvent and stable in the following filtration experiments, which will be discussed later. The introduction of carboxyl group (SA) will be helpful to understand the effect of the charge state of the obtained nanofiber membrane. The synthesis and characterization of PEA and SA-PEA containing coumarin units can be found in the ESI (Scheme S1 and Fig. S1†). The poly(ether amine) solution (PEA or SA-PEA) was electrospun from a syringe to produce a nanofiber membrane. By controlling the electrospun polymer

concentration (a solid content of 50% in DMF solution) and the electrospinning conditions (an applied voltage of 17 kV with the flow rate of 0.2 mL h^{-1}), we can obtain the nanofibers of PEA and SA-PEA with uniform diameter and smooth surface, whose morphology is revealed by SEM (Fig. 1b and e). The diameter of both PEA and SA-PEA nanofibers is around 330 nm, and the morphology kept almost unchanged after irradiation of UV-light. The diameter uniformity and absence of beads in the obtained electrospun nanofibers is important in the fabrication of a nanofiber membrane with good performance.

Due to the presence of coumarin moieties in the PEA chain, the obtained PEA and SA-PEA nanofibers can be further crosslinked through UV-light induced dimerization. The process of photo-dimerization of coumarin was traced by both diffuse reflectance UV-vis spectra and FT-IR (Fig. 2). As shown in Fig. 2a, upon the exposure of 365 nm UV light, the peak ascribed to the adsorption of coumarin units decreased gradually suggesting the dimerization of coumarin. The FT-IR spectra at different irradiation times also confirm the photo-dimerization of coumarin groups. The peak of C=O in coumarin units (1726 cm^{-1}) shifts to the left at 1765 cm^{-1} . The photo-dimerization can weaken the conjugation effect of coumarin, resulting in the increased stretching vibration energy of C=O and left-shift of the C=O peak.

Upon irradiation of UV light for about 2 h, the photo-dimerization of coumarin moieties to become dimers can make the nanofiber membrane cross-linked. The corresponding SEM images of the cross-linked PEA and SA-PEA nanofiber membranes are shown in Fig. 1. No obvious difference was found to either PEA or SA-PEA nanofibers before and after cross-linking. The cross-linked nanofibers also keep the uniform

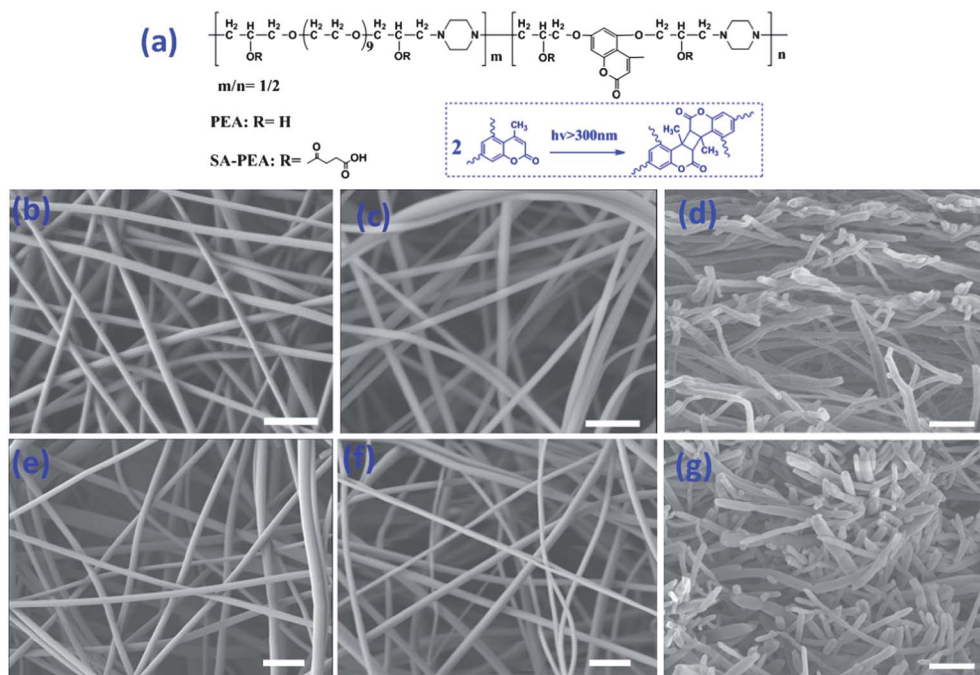


Fig. 1 (a) Chemical structure of PEA and SA-PEA and the photo-dimerization of coumarin; SEM images of PEA and SA-PEA nanofiber membranes: (b) PEA-NF before cross-linking; (c) PEA-NF after cross-linking; (d) cross-sectional image of PEA-NF after cross-linking; (e) SA-PEA-NF before cross-linking; (f) SA-PEA-NF after cross-linking; (g) cross-sectional image of SA-PEA-NF after cross-linking. The scale bar is 2 μm.

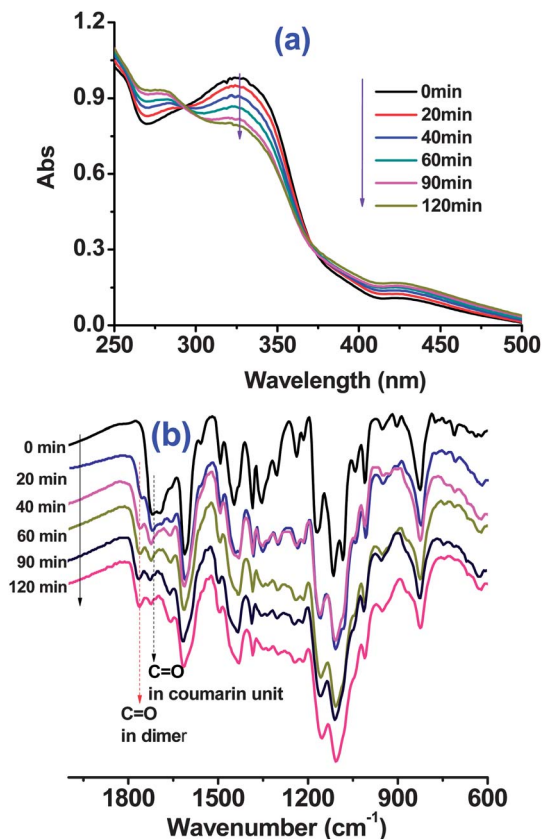


Fig. 2 Characterization of PEA-NF photo-dimerization kinetics. (a) Diffuse reflectance ultraviolet visible spectra of PEA-NF membrane after UV irradiation; (b) the FT-IR spectra and C=O shift after UV irradiation.

diameter and smooth surface, and interconnect with each other to form a mesh structure in the membrane. As a result of cross-linking, the PEA nanofiber membrane is expected to be stable even if in good solvents. This is indeed true and confirmed by the SEM images shown in Fig. 3. After being immersed in solvents such as tetrahydrofuran (THF), toluene and chloroform at room temperature for 24 h, all of which are good solvents for PEA, the cross-linked PEA nanofibers still maintained their fiber morphology and integrity. The average diameter of cross-linked PEA-NF increased slightly after immersion to some extent, which may be ascribed to the swelling of PEA-NF in solvents (Fig. 3d). The remarkable solvent resistance of cross-linked PEA-NF membrane can be explained by both intra and inter-nanofiber cross-linking, which was induced by the photo-dimerization of coumarin moieties. The intra-nanofiber cross-linking can make PEA-NF keep its fibrous morphology, while the inter-nanofiber cross-linking is helpful to dimensional stability of the nanofiber membrane. The excellent stability of PEA nanofiber membrane is of vital importance in the following adsorption and filtration experiments.

Selective adsorption behavior of hydrophilic dyes

The adsorption behavior of the two cross-linked PEA nanofiber membranes to nine hydrophilic dyes was first investigated, as

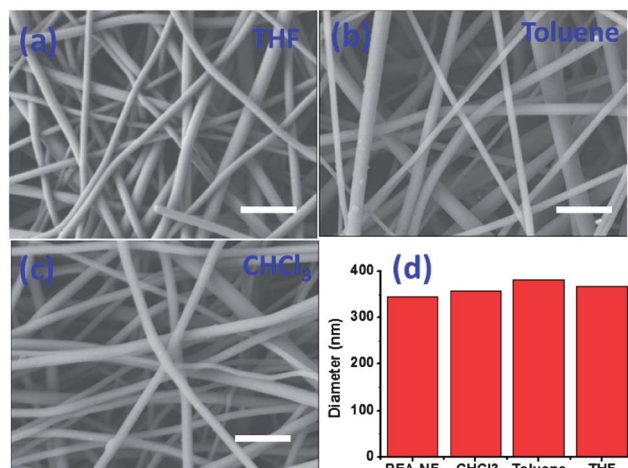


Fig. 3 SEM images of photo-crosslinked PEA-NF after being immersed in organic solvents (a) THF, (b) toluene, (c) CHCl_3 and (d) their corresponding average diameters. The scale bar is $2 \mu\text{m}$.

well as the bulk gel of PEA as reference. The structures and abbreviations of these hydrophilic dyes are listed in Fig. 4, and they can be divided into three types: fluorescein dyes including RB, Cal, and FR; azo dyes including OG, PSX, PS, and BY and other dyes including R6G and MB. The adsorption experiments were conducted in aqueous solution, in which the initial concentration of dyes and PEA adsorbents were fixed at $200 \mu\text{M}$ and 3.3 mg mL^{-1} , respectively. After addition of PEA-NF for 12 h, the color of RB, PS, PSX and OG solutions turned obviously light, while R6G and MB solutions remained almost unchanged (Fig. S2†).

Taking OG and MB as examples, it can be seen with the naked eye that most of the OG was adsorbed by PEA-NF, but MB still stayed in solution (Fig. 5a). UV-vis spectra of dye solutions before and after adding PEA-NF for 12 h were recorded for the adsorption of dyes (Fig. 5a). More than 96% OG was adsorbed by PEA-NF membrane, while less than 5% MB was adsorbed. The saturated adsorption capacity (Q_{eq}), which is an important parameter for an adsorbent in practical applications, was determined by UV-vis spectra. PEA nanofibers and gel exhibited high Q_{eq} to OG, PS, PSX and RB regardless of charge states of both adsorbent and dye, while they possessed low Q_{eq} to R6G and MB (Fig. 5b). The large difference in Q_{eq} suggests the selective adsorption of PEA-NF to the hydrophilic dyes. The adsorption behavior of PEA-NF to these nine hydrophilic dyes is almost the same to that of SA-PEA-NF, suggesting that the electrostatic interaction between the host PEA-NF and the guest dyes has no obvious effect on adsorption. This is the same to our previous reports about the selective adsorption behavior of PEA-based hydrogel to hydrophilic dyes. We also found that Q_{eq} of PEA-NF to most dyes is much higher than that of PEA-Gel, which can be explained by the advantage of high surface-to-volume ratio of nanofibers.

We studied the adsorption kinetics of the nine dyes to further understand the interaction between PEA-NF and dyes (Fig. 6). For the dyes with high Q_{eq} such as RB, OG, PSX, BY and PS, the adsorption capacity increased rapidly initially and then

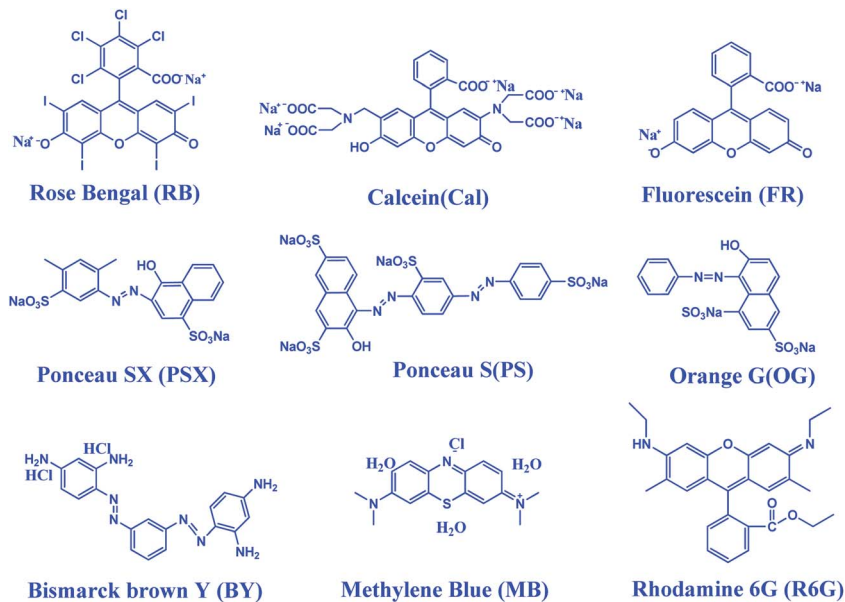


Fig. 4 Chemical structures and abbreviations of the nine hydrophilic dyes.

continued to increase with the contact time at a relatively slow rate. On the contrary, the adsorption rate and capacity of R6G and MB are much lower regardless of their charge states,

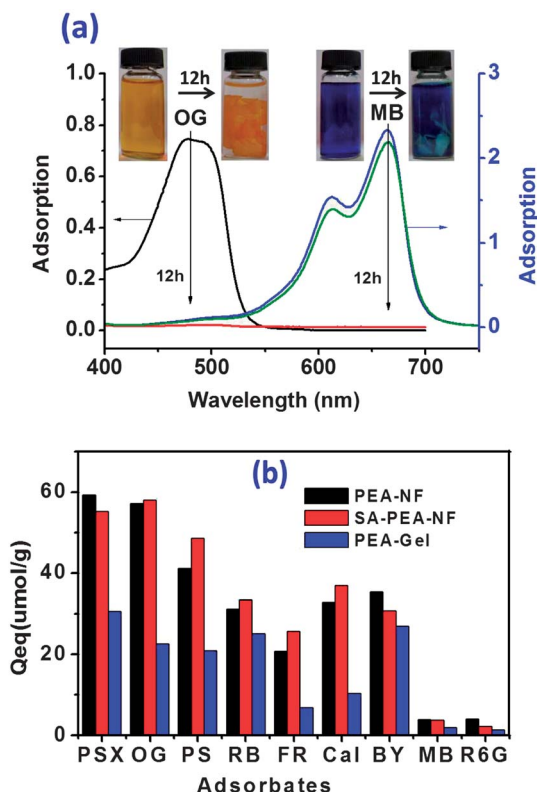


Fig. 5 (a) UV-vis spectra of OG and MB before and after adsorption by PEA-NF for 12 h. Inset pictures are photos of solutions of OG and MB before and after adsorption by PEA-NF for 12 h. (b) Saturated adsorption capacities of PEA-NF, SA-PEA-NF and PEA-Gel for dyes at 25 °C. 20 mg of adsorbent was added into 6 mL of the dyes' aqueous solutions and the initial dye concentration is 200 μM.

indicating further that the electrostatic interaction does not affect the adsorption behavior of PEA-NF. This was also supported by the fact that PEA-NF possesses similar adsorption kinetics of the nine dyes to SA-PEA-NF. Compared with PEA-Gel, PEA nanofiber membranes (PEA-NF and SA-PEA-NF) exhibited faster adsorption rates and higher adsorption capacities, which is consistent with the experiments of the saturated adsorption capacity (Q_{eq}) and confirms that nanofibers with high surface-to-volume ratio possess a great advantage in adsorption. To investigate the adsorption mechanism of dyes onto the PEA-NF, we used a pseudo-second-order equation to analyze the adsorption kinetics (Fig. S3†). The kinetic parameters, the pseudo-second-order adsorption rate constant (k), the experimental and calculated adsorption capacity ($Q_{eq,exp}$ and $Q_{eq,cal}$), the correlation coefficient (R^2), are summarized in Table S1.† The high correlation coefficient (R^2 is close to 1.0) and the almost same values of $Q_{eq,exp}$ and $Q_{eq,cal}$ indicated that the pseudo-second-order model applied well to the adsorption of dyes onto PEA-NF. It is easily understood that k and Q_{eq} can reflect the strength of interaction between PEA-NF and dyes: large values of k and Q_{eq} mean a strong affinity. The difference of k and Q_{eq} suggested that PEA-NF possessed unique selective adsorption to the hydrophilic dyes, as well as PEA-based hydrogel.

Separation of dyes by molecular filtration

The characteristics of unique selective and fast adsorption to dyes, and cross-linked structure resistance to solvent make PEA nanofibers have possible applications in the separation of hydrophilic dyes in aqueous solution through molecular filtration. We evaluated the filtration performances of PEA-NF and SA-PEA-NF by filtering aqueous solutions of the nine dyes, and the breakthrough curves are shown in Fig. 7. The dye aqueous solutions with a concentration of 11 μM were passed through the PEA nanofiber membranes (10 mg) with the flow rate of

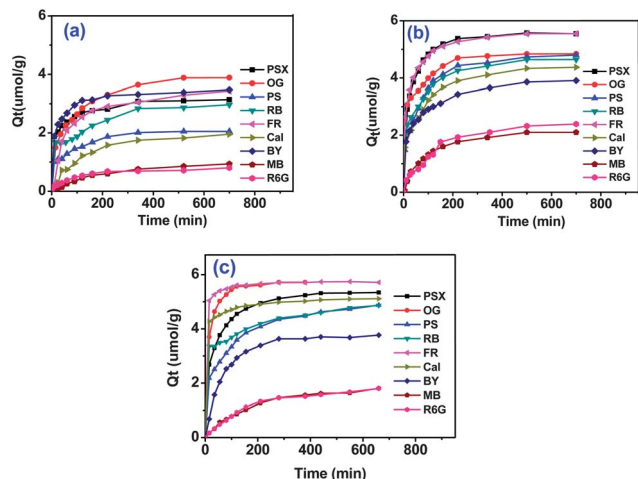


Fig. 6 Adsorption capacity Q_t versus time curves for the adsorption of nine dyes, RB, Cal, FR, OG, PSX, PS, BY, R6G and MB, onto (a) PEA-Gel, (b) PEA-NF, (c) SA-PEA-NF at 25 °C.

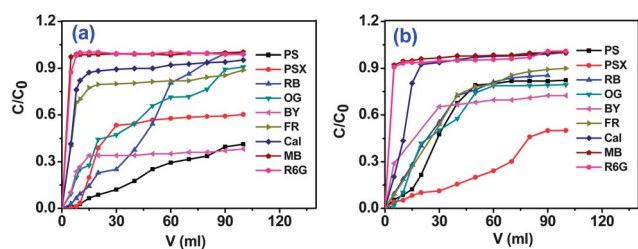


Fig. 7 Breakthrough curves for the passage of the nine dye solutions through (a) PEA-NF membrane and (b) SA-PEA-NF membrane: the ratio of dye concentration between filtrate and original solution is plotted as a function of filtrate volume. Flow rate 3.0 mL min^{-1} , and mass of PEA-NF and SA-PEA-NF is 10 mg. Initial dye concentration is $11 \mu\text{M}$.

3.0 mL min^{-1} . We failed in the filtration experiment of the reference PEA-Gel membrane because of its low permeation of water, which might be caused by the non-porous structure. PEA-NF exhibited different filtration performance towards the nine

dye solutions, which coincides with the results of the adsorption kinetics. In the curves of MB and R6G solutions with low Q_{eq} and slow adsorption rate, the outlet concentration reached the feed concentration very rapidly (Fig. 7a). The MB and R6G concentration of the first 5 mL effluent from PEA-NF membrane is nearly close to their original concentration, indicating that the PEA-NF membrane did not capture MB and R6G. In contrast, most of PS and PSX were removed when their aqueous solutions passed through the PEA-NF membrane. The concentration of dye in the filtrate is only half of the feed concentration when the effluent reached 100 mL, which should be caused by the strong and fast adsorption of PS and PSX by PEA-NF membrane. There are no obvious differences in breakthrough curves between PEA-NF and SA-PEA-NF membranes, suggesting that electrostatic interaction has only a slight effect on the filtration behavior. This is in good agreement with the selective adsorption of PEA nanofiber membrane to hydrophilic dyes.

The above adsorption and filtration experiments reveal that PEA nanofiber membranes can be used in separation of a dye mixture through filtration. When an aqueous solution of dye mixture passes through a PEA nanofiber membrane, dyes with strong affinity to PEA nanofibers such as PS, and PSX will be removed from the aqueous solution, while MB and R6G with low Q_{eq} are expected to remain in the filtrate. Taking a mixture of PS/MB as an example, 200 mL solution mixture (concentrations of PS and MB are $5.5 \mu\text{M}$) was forced to pass through PEA-NF membrane (the diameter and weight of membrane are about 4 cm and 30 mg, respectively) at different flow rates. As shown in Fig. 8a and Movie S1,[†] good separation results can be achieved even if at a high flow rate of 60 mL min^{-1} ($2870 \text{ L m}^{-2} \text{ h}^{-1}$). Almost all of the PS was captured by the PEA-NF membrane, while the color of the filtrate became the blue of MB aqueous solution. The concentrations of PS and MB in the filtrate were determined by UV-vis spectra (Fig. 8b). The concentration of PS in the filtrate decreased from the initial 5.5 to $0.2 \mu\text{M}$, which is about 7% of the concentration of MB ($5.0 \mu\text{M}$) in the filtrate. In other words, the purity of MB in the filtrate is about 93% after filtration. We tried a higher flow rate (100 mL min^{-1}) and the purity of MB in the filtrate is about 83% after filtration (Fig. S4[†]), which might be due to the reduced residence time.

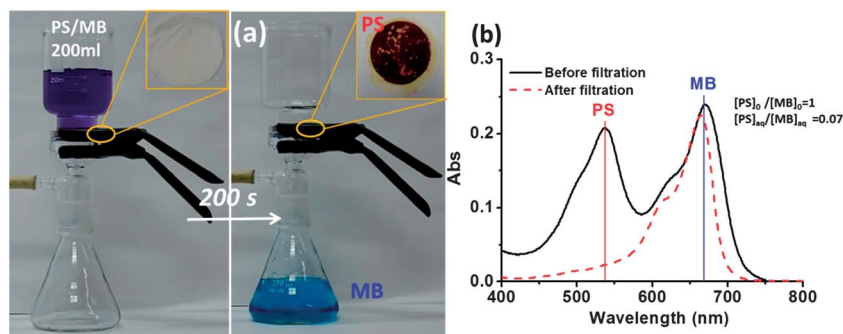


Fig. 8 Separation of mixed dyes PS/MB by PEA-NF membrane. (a) Equipment for molecular filtration and photographs before and after filtering PS/MB solution, and inset is the photograph of PEA-NF membrane before and after adsorbing PS; (b) UV-vis spectra of PS/MB solution before and after filtration at a flow rate of 60 mL min^{-1} . The volume of PS/MB solution mixture with the concentration of $5.5 \mu\text{M}$ is 200 mL, and the diameter and weight of membrane are about 4 cm and 30 mg, respectively.

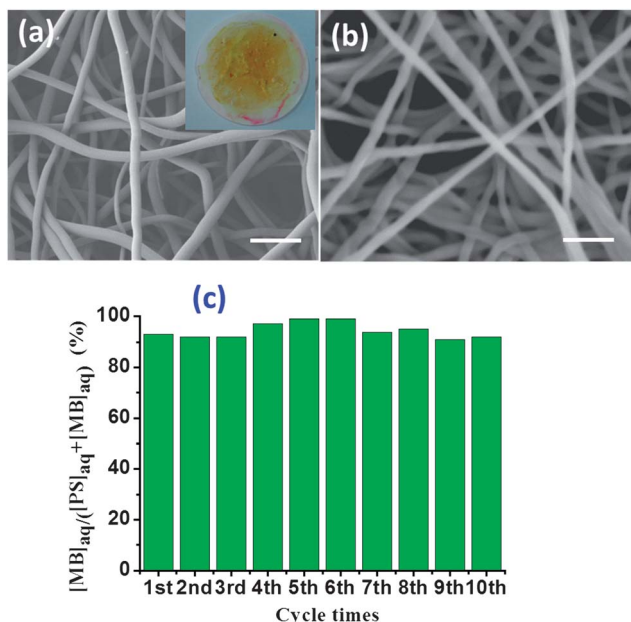


Fig. 9 Regeneration and reusability tests for PEA-NF membrane. (a) SEM image and photo of the regenerated PEA-NF membrane for the first time. (b) SEM image of PEA-NF membrane after 10 continuous filtration separation experiments. (c) Separation efficiency by the regenerated PEA-NF membrane at different recycle times. Separation efficiency is defined as $[MB]_{aq}/([PS]_{aq} + [MB]_{aq})$. The scale bar in (a) and (b) is 2 μm .

SEM observation revealed that the PEA-NF membrane after filtration kept almost the same morphology to that before filtration, suggesting the good stability of PEA-NF membrane (Fig. S5a and b†). We also conducted the separation of another mixture of BY/MB through the same approach (Fig. S6†). The concentration of BY is about 7% of the concentration of MB in the filtrate when the flow rate is as high as 60 mL min^{-1} .

The reusability of PEA-NF membrane was also evaluated because it is important to recycle PEA-NF membranes for practical application. With the same filtration equipment, PS adsorbing PEA-NF membrane can be regenerated by NaOH aqueous solution (1 mg mL^{-1}). As shown in Fig. 9a, the red PEA-NF membrane became light yellow after being washed by NaOH aqueous solution, indicating that PS was washed off from PEA-NF membrane. SEM images revealed that PEA-NF kept the fibrous morphology after the first generation. In the complete continuous filtration–regeneration tests, PEA-NF membrane can separate the mixture of PS/MB with high efficiency, and the purity of MB in the filtrate can reach 95% even in the 10th cycle (Fig. 9c). This should be ascribed to the good stability of PEA-NF membrane, which was confirmed by the fibrous morphology of PEA-NF after ten times' regeneration (Fig. 9b and S5c†).

3. Conclusion

In summary, a novel nanofiber membrane of poly(ether amine) is reported, which is able to separate a mixture of hydrophilic dyes in aqueous solution through facile filtration. The PEA-NF

membranes fabricated through electrospinning technology can be cross-linked through photo-induced dimerization of coumarin units in the PEA chain, and consequently were stable and resistant to solvents. Regardless of their charge state, PEA-NF membranes possess unique selectivity in the adsorption of hydrophilic dyes: PEA-NF membranes have quick adsorption to PS, PSX, OG and RB with high Q_{eq} and slow adsorption to MB and R6G with low Q_{eq} . These novel characteristics, such as the unique selective and fast adsorption to the hydrophilic dyes, and stability in solvents, make PEA-NF membrane successful in the separation of PS/MB in aqueous solution through the molecular filtration with a very high flux rate of $2870 \text{ L m}^{-2} \text{ h}^{-1}$. In addition, the PEA-NF membranes are easily regenerated and maintain their high separation efficiency over ten filtration–regeneration cycles. It is believed that PEA-NF membranes will find potential in the fields of molecular filtration, such as separation and water purification.

4. Experimental

Fabrication of PEA and SA-PEA NF by electrospinning

A certain amount of PEA or SA-PEA was dissolved in DMF at a concentration of 50% (wt%). The mixture was stirred for 2 h before electrospinning. The prepared solution of PEA or SA-PEA was transferred into a plastic syringe and fed through the metal needle at a feeding rate of 0.2 mL h^{-1} . The voltage used for electrospinning was 17 kV, and the distance between the metal needle and the collecting plate was kept at 12 cm. A square metallic collecting plate covered with aluminium foil was applied for the fiber deposition. The nanofibers by electrospinning were photo-crosslinked after irradiating for 2 h by 365 nm UV light. In comparison, a certain amount of PEA was dissolved in DMF. Then the prepared solution was poured onto the polytetrafluoroethylene matrix to form a circular PEA-Gel.

Characterization

¹H-NMR spectra with DMF as the solvent were acquired by a Mercury Plus spectrometer (Varian, Inc., USA) operating at 400 MHz and using TMS as an internal standard at room temperature.

Fourier transform infrared spectroscopy (FT-IR) spectra of PEA-NF were recorded on a Nicolet iS10 FT-IR spectrometer (Thermo Scientific, USA). Diffuse reflectance ultraviolet visible spectra were obtained using a Perkin-Elmer Lambda 750S UV-vis Spectrometer. The samples at different irradiation times were prepared by sticking the PEA fiber membrane onto a white paper whose diffuse reflectance UV-vis spectrum was collected as the background. The two methods were used to examine the photo-crosslinking kinetics of PEA-NF.

Scanning electron microscopy (SEM) was carried out on a JSM-7401F electron microscope (JEOL, Japan) at 5 kV, which showed the sizes and images of the nanofibers. All the fiber membranes were coated with gold particles for observation.

Adsorption experiments

Nine hydrophilic dyes were chosen for the adsorption experiments. Their structures are shown in Fig. 4. All the dyes'

concentrations were measured from the dyes' calibration curves. The corresponding UV-vis spectra of dyes were recorded with a UV-2550 spectrophotometer.

The adsorption kinetics tests were conducted with an initial dye concentration of 30 μM , and the volume of the dyes is 4 mL. 20 mg membranes including PEA-NF, SA-PEA-NF, and PEA-Gel, were immersed in the prepared dye solution. The adsorption capacity was evaluated by UV-vis spectra at different adsorption times.

Saturated adsorption experiments were performed under the same conditions as above except for the dye concentration which was 200 μM in a total volume of 6 mL. The three adsorbents (PEA-NF, SA-PEA-NF, PEA-Gel) were respectively immersed in the dyes for 12 h to reach their adsorption equilibrium. The equilibrium adsorption capacity (Q_{eq}) of dyes is defined as follows:

$$Q_{\text{eq}} = \frac{(C_0 - C_{\text{eq}})}{M} V \quad (1)$$

where Q_{eq} ($\mu\text{mol g}^{-1}$) is the amount of adsorbed dyes per gram of adsorbent at equilibrium, C_0 is the initial concentration of dyes in the solution ($\mu\text{mol L}^{-1}$), C_{eq} is the concentration of dyes at equilibrium ($\mu\text{mol L}^{-1}$), V is the volume of the solution (L), and M is the mass of the adsorbent used (g).

The adsorption behaviors were also traced by UV-vis spectra and calculated at the maximum adsorption from the dyes' calibration curves.

Breakthrough curves of dyes through PEA NF membrane

The equipment for filtration is the general silica sand filtration unit. The experiment was performed with 10 mg PEA-NF membrane (diameter = 4 cm) and 100 mL dyes at a concentration of 11 $\mu\text{mol L}^{-1}$. The flow rate of dye solution was controlled at 3 mL min^{-1} using a vacuum pump. Then a UV-2550 spectrophotometer was applied to measure the concentration of dyes having been filtered through PEA-NF at different filtration volumes. After calculations and analysis, we could get the breakthrough curves of dyes through our PEA-NF membrane.

Molecular filtration separation of mixed dyes

The separation experiments were conducted by way of filtration. The equipment used for filtration is the same as the one for breakthrough experiments. A piece of PEA-NF membrane with a diameter of 4 cm and mass of 30 mg was placed in the unit. The mixed dyes of PS/MB, and BY/MB with a concentration of 5.5 μM were forced to flow through the PEA-NF membrane at various flow rates (60–100 mL min^{-1}) using the vacuum pump as the controller. The whole experimental process of PS/MB separation was taken as a video by a camera. The separation efficiency (η) was defined as the follows:

$$\eta = \frac{[\text{MB}]_{\text{aq}}}{[\text{MB}]_{\text{aq}} + [\text{PS}]_{\text{aq}}} \times 100\% \quad (2)$$

where $[\text{MB}]_{\text{aq}}$ and $[\text{PS}]_{\text{aq}}$ are the concentrations of MB and PS in the filtrate, respectively.

Regeneration of PEA-NF membrane

After the above separation experiment of PS/MB, the PEA-NF membrane having adsorbed PS could be regenerated by the washing of NaOH aqueous solution. The NaOH aqueous solution (1 mg mL^{-1}) was loaded at 60 mL min^{-1} to elute PS, resulting in the regeneration of PEA-NF membrane. In order to evaluate the performance of the regenerated PEA-NF membrane, it was used to separate PS/MS (5.5 μM) solution every time after the PEA-NF membrane was regenerated. The PEA-NF membrane for the regeneration experiments is 30 mg. The above cycle was repeated for 10 continuous runs to assess the PEA-NF membrane's performance.

Acknowledgements

We thank the National Nature Science Foundation of China (21174085, 21274088), Science & Technology and Education Commission of Shanghai Municipal Government (12ZZ020), and the Shanghai Leading Academic Discipline Project (B202) for their financial support. X. S. Jiang is supported by the NCET-12-3050 Project.

References

- 1 I. Soroko, Y. Bhole and A. G. Livingston, *Green Chem.*, 2011, **13**, 162–168.
- 2 P. Vandezande, L. E. M. Gevers and I. F. J. Vankelecom, *Chem. Soc. Rev.*, 2008, **37**, 365–405.
- 3 A. Nykanen, M. Nuopponen, A. Laukkanen, S. P. Hirvonen, M. Rytela, O. Turunen, H. Tenhu, R. Mezzenga, O. Ikkala and J. Ruokolainen, *Macromolecules*, 2007, **40**, 5827–5834.
- 4 H. B. Park, C. H. Jung, Y. M. Lee, A. J. Hill, S. J. Pas, S. T. Mudie, E. Van Wagner, B. D. Freeman and D. J. Cookson, *Science*, 2007, **318**, 254–258.
- 5 J. Han, J. Fu and R. B. Schoch, *Lab Chip*, 2008, **8**, 23–33.
- 6 D. L. Gin and R. D. Noble, *Science*, 2011, **332**, 674–676.
- 7 J. Shang, G. Li, R. Singh, Q. F. Gu, K. M. Nairn, T. J. Bastow, N. Medhekar, C. M. Doherty, A. J. Hill, J. Z. Liu and P. A. Webley, *J. Am. Chem. Soc.*, 2012, **134**, 19246–19253.
- 8 B. J. Hinds, N. Chopra, T. Rantell, R. Andrews, V. Gavalas and L. G. Bachas, *Science*, 2004, **303**, 62–65.
- 9 H. L. Casticum, G. G. Paradis, M. C. Mittelmeijer-Hazeleger, R. Kreiter, J. F. Vente and J. E. ten Elshof, *Adv. Funct. Mater.*, 2011, **21**, 2319–2329.
- 10 F. Zhang, X. Zou, X. Gao, S. Fan, F. Sun, H. Ren and G. Zhu, *Adv. Funct. Mater.*, 2012, **22**, 3583–3590.
- 11 C. Aydiner, Y. Kaya, Z. Beril Gnder and I. Vergili, *J. Chem. Technol. Biotechnol.*, 2010, **85**, 1229–1240.
- 12 T. Uyar, R. Havelund, J. Hacaloglu, F. Besenbacher and P. Kingshott, *ACS Nano*, 2010, **4**, 5121–5130.
- 13 I. Tokarev and S. Minko, *Adv. Mater.*, 2010, **22**, 3446–3462.
- 14 T. R. Gaborski, J. L. Snyder, C. C. Striemer, D. Z. Fang, M. Hoffman, P. M. Fauchet and J. L. McGrath, *ACS Nano*, 2010, **4**, 6973–6981.
- 15 Y. Han, Z. Xu and C. Gao, *Adv. Funct. Mater.*, 2013, **29**, 3693–3700.

- 16 C. Gao, Z. Sun, K. Li, Y. Chen, Y. Cao, S. Zhang and L. Feng, *Energy Environ. Sci.*, 2013, **6**, 1147–1151.
- 17 J. H. Kim, M. Abouelnasr, L. C. Lin and B. Smit, *J. Am. Chem. Soc.*, 2013, **135**, 7545–7552.
- 18 K. Li, D. H. Olson, J. Y. Lee, W. Bi, K. Wu, T. Yuen, Q. Xu and J. Li, *Adv. Funct. Mater.*, 2008, **18**, 2205–2214.
- 19 S. B. Lee, D. T. Mitchell, L. Trofin, T. K. Nevanen, H. Söderlund and C. R. Martin, *Science*, 2002, **296**, 2198–2200.
- 20 S. P. Nunes, R. Sougrat, B. Hooghan, D. H. Anjum, A. R. Behzad, L. Zhao, N. Pradeep, I. Pinnau, U. Vainio and K. V. Peinemann, *Macromolecules*, 2010, **43**, 8079–8085.
- 21 H.-T. Wong, Y. H. See-Toh, F. C. Ferreira, R. Crook and A. G. Livingston, *Chem. Commun.*, 2006, 2063–2065.
- 22 P. T. Witte, S. R. Chowdhury, J. E. ten Elshof, D. Sloboda-Rozner, R. Neumann and P. L. Alsters, *Chem. Commun.*, 2005, 1206–1208.
- 23 M. A. Shannon, P. W. Bohn, M. Elimelech, J. G. Georgiadis, B. J. Marinas and A. M. Mayes, *Nature*, 2008, **452**, 301–310.
- 24 V. Thavasi, G. Singh and S. Ramakrishna, *Energy Environ. Sci.*, 2008, **1**, 205–221.
- 25 N. Wang, X. Wang, B. Ding, J. Yu and G. Sun, *J. Mater. Chem.*, 2012, **22**, 1445–1452.
- 26 K. Yoon, B. S. Hsiao and B. Chu, *J. Mater. Chem.*, 2008, **18**, 5326–5334.
- 27 Q. Zhang, E. Uchaker, S. L. Candelaria and G. Cao, *Chem. Soc. Rev.*, 2013, **42**, 3127–3171.
- 28 S. Wu, F. Li, Y. Wu, R. Xu and G. Li, *Chem. Commun.*, 2010, **46**, 1694–1696.
- 29 M. Henmi, K. Nakatsuji, T. Ichikawa, H. Tomioka, T. Sakamoto, M. Yoshio and T. Kato, *Adv. Mater.*, 2012, **24**, 2238–2241.
- 30 W. Zhang, Z. Shi, F. Zhang, X. Liu, J. Jin and L. Jiang, *Adv. Mater.*, 2013, **25**, 2071–2076.
- 31 M. B. Shiflett and H. C. Foley, *Science*, 1999, **285**, 1902–1905.
- 32 J. K. Holt, H. G. Park, Y. Wang, M. Stadermann, A. B. Artyukhin, C. P. Grigoropoulos, A. Noy and O. Bakajin, *Science*, 2006, **312**, 1034–1037.
- 33 X. B. Ke, H. Y. Zhu, X. P. Gao, J. W. Liu and Z. F. Zheng, *Adv. Mater.*, 2007, **19**, 785–790.
- 34 K. B. Jirage, J. C. Hulteen and C. R. Martin, *Science*, 1997, **278**, 655–658.
- 35 E. Kharlampieva, V. Kozlovskaya, J. Tyutina and S. A. Sukhishvili, *Macromolecules*, 2005, **38**, 10523–10531.
- 36 C. C. Striemer, T. R. Gaborski, J. L. McGrath and P. M. Fauchet, *Nature*, 2007, **445**, 749–753.
- 37 J. R. Ku and P. Stroeve, *Langmuir*, 2004, **20**, 2030–2032.
- 38 R. B. Schoch, A. Bertsch and P. Renaud, *Nano Lett.*, 2006, **6**, 543–547.
- 39 H.-W. Liang, X. Cao, W.-J. Zhang, H.-T. Lin, F. Zhou, L.-F. Chen and S.-H. Yu, *Adv. Funct. Mater.*, 2011, **21**, 3851–3858.
- 40 P. Chen, H. W. Liang, X. H. Lv, H. Z. Zhu, H. B. Yao and S. H. Yu, *ACS Nano*, 2011, **5**, 5928–5935.
- 41 Z. Lai, G. Bonilla, I. Diaz, J. G. Nery, K. Sujaoti, M. A. Amat, E. Kokkoli, O. Terasaki, R. W. Thompson, M. Tsapatsis and D. G. Vlachos, *Science*, 2003, **300**, 456–460.
- 42 R. Wang, B. Yu, X. Jiang and J. Yin, *Adv. Funct. Mater.*, 2012, **22**, 2606–2616.
- 43 B. Li, X. Jiang and J. Yin, *J. Mater. Chem.*, 2012, **22**, 17976–17983.
- 44 S. J. Deng, H. J. Xu, X. S. Jiang and J. Yin, *Macromolecules*, 2013, **46**, 2399–2406.
- 45 S. Deng, R. Wang, H. Xu, X. Jiang and J. Yin, *J. Mater. Chem.*, 2012, **22**, 10055–10061.